# Analysis of an air-spaced patch antenna near 1800 MHz

Hermine Nathalie Akouemo Kengmo Kenfack
*Marquette University*

# ANALYSIS OF AN AIR-SPACED PATCH ANTENNA NEAR 1800 MHz

by

Hermine N. Akouemo Kengmo Kenfack, B.S.

A Thesis submitted to the Faculty of the Graduate School,
Marquette University,
in Partial Fulfillment of the Requirements
for the Degree of Master of Science.

Milwaukee, WI

December 2011

ABSTRACT

ANALYSIS OF AN AIR-SPACED PATCH ANTENNA NEAR 1800 MHz

Hermine N. Akouemo Kengmo Kenfack, B. S.

Marquette University, 2011

Microstrip antennas are a type of printed antenna which consists of a patch on top of a grounded substrate. A major limitation for the performance of the patch antenna is the dielectric substrate. The idea of using air as dielectric was therefore considered to overcome that limitation because air has the lowest permittivity and no loss. The goal of this work is to build an air-spaced patch antenna, with the minimum resonant frequency at 1800 MHz and with a return loss of at least 10 dB.

This work is novel because the air-spaced patch antenna has not been extensively studied. Existing literature on patch antennas with dielectric were used for the design of the antenna (dimensions of the patch, ground plane and height) and to understand the principles of operation of microstrip patch antennas in general. Simulations using the NEC code and experiments in the RF laboratory were used for this air-spaced patch antenna study.

The Numerical Electromagnetic Code (NEC) was used as the simulation tool in this work. The air-spaced patch antenna was simulated to find a trend for the variation of the return loss and impedance with the resonant frequency. Simulation also helped determine cases that will not be meaningful to explore in the experiment.

The experiment was done in the RF laboratory of Marquette University College of Engineering. Two procedures were used to calculate the patch dimensions using two different sources ([2], [3]). They lead to two patch antennas that were tested. For each antenna, the height of the dielectric substrate and the recess feed distance were varied. Antenna 2 (procedure 2 - [3]) provided the best results with a resonant frequency of 1800 MHz and a return loss of 21 dB.

It was found that the error between experimental and simulation resonant frequency is generally 5% or less. This error increases as the dielectric height increases, and as the recess distance increases. Simulation results roughly follow the experimental results trend.

# ACKNOWLEDGEMENTS

Hermine N. Akouemo Kengmo Kenfack, B. S.

I would like to thank all my family for their sacrifices, love and unending support. I would like to thank Dr. Richie for his assistance and guidance throughout these two years and this work. I would like to thank Dr. Luglio for being on my committee and for attending every seminar presentation on my work. I would like to thank Dr. Yaz for also being on my committee. I would also like to thank Dr. Wolski and Dr. Ishii for providing helpful and meaningful insights for this work. Last by not least, I would like to thank the Microwave seminar attendees, for providing meaningful feedback, advice and ideas on this work. It has been an amazing journey for me and thank you to the Marquette University College of Engineering professors.

# TABLE OF CONTENTS

# LIST OF TABLES

# LIST OF FIGURES

# Chapter I - Introduction

## I.1 Motivation

A microstrip patch antenna is a type of printed antenna which, in its simplest form, consists of a layered structure with two parallel conductors separated by a thin dielectric substrate. The lower conductor acts as a ground plane and the upper conductor acts as the radiator (fraction of a wavelength in extent) [2].

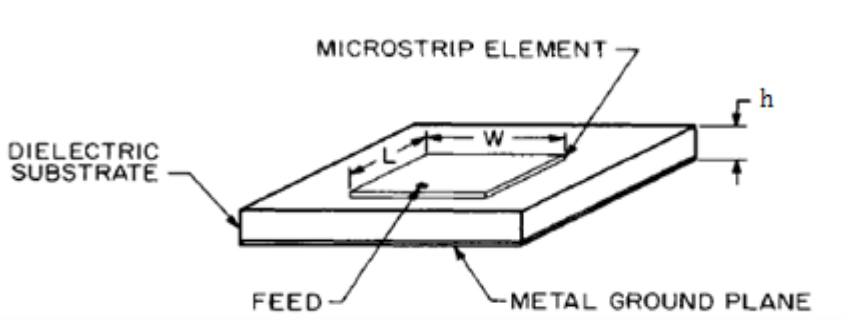


Figure 1: Rectangular microstrip patch structure [2]

Patch antennas can be in many different shapes. The rectangular patch antenna is the simplest configuration of microstrip patch antennas. Rectangular patch antennas are very easy to fabricate. They can be used for a variety of applications: satellite communications, radars, command and control, feed element in complex antenna fabrication, biomedical radiator, etc. Microstrip antennas can also be used for many military and commercial devices, such as use on aircraft or space antennas.

There is an increasing demand for the use of microstrip antennas in wireless communications due to their inherently low back radiation, ease of conformity and high gain as compared to wire antennas. Microstrip antennas are used in cellular phones, telecommunications applications in general (base station, radio, etc), TV, Radio, etc. Arrays of microstrip antennas are used in broadcast satellite receiver antennas to achieve an increase of bandwidth [5]. In satellite communications, the design of the microstrip antenna reported at S-band for remote sensing satellites can be adapted to provide the circularly polarized conical patterns required for effective data transmission between the satellite and earth at both UHF and S-band frequencies [8]. Microstrip antennas are also used as feed element in complex antennas and they are used in Doppler and other radar applications. This list of applications of microstrip antennas is not exhaustive. The number of applications increases with the increases in advantages and awareness of possibilities of microstrip antennas.

Microstrip antennas became popular around 1970 [2] due to availability of good substrates and better theoretical models. They can be of various shapes depending on the applications and the type of polarization to be achieved. Linear and circular polarizations are easy to achieve with simple changes in feed position and the antennas can operate in dual frequency mode.

Microstrip antennas have several advantages compared to conventional microwave antennas. Some of the principal advantages of microstrip antennas are:

- Lightweight, low volume and thin profile configurations, which can be made conformal
- Low fabrication cost; mass production is easy with this type of product

- Linear and circular polarization are possible with simple changes in feed position
- Can be easily integrated in other microwave circuits
- No cavity backing is required
- Dual frequency and dual polarization antennas can be easily made

However, microstrip antennas also have disadvantages compared to conventional microwave antennas including:

- Narrow bandwidth
- Low efficiency (loss can sometimes considerably reduce the gain)
- Poor scan performance (most microstrip antennas radiate into a half plane)
- Poor isolation between the feed and the radiating elements.
- Lower power handling capability (maximum roughly 100W)

Microstrip patch antennas can be of various geometrical shapes (rectangle, disk, square, ellipse, etc.). The most widely used configuration is the rectangular one because of the simplicity of its structure.

## I.2 Problem statement

Microstrip patch antennas usually have a dielectric between the patch itself and the ground plane, which reduces the efficiency of the antenna. Using a dielectric with low permittivity and low loss tangent is one way of improving the efficiency of the antenna and widening the bandwidth. Generally foam is used as dielectric substrate with the lowest dielectric constant for patch antennas. Foam has a dielectric constant of 1.03 and very low dielectric loss factors (tan $\delta$=0.0008), but the surface of the foam is not well defined, which makes it impractical to deposit material directly on it. Foam is also a

porous material. Therefore, the idea of using air as the dielectric is investigated here. Air is a dielectric with permittivity of 1 and with loss tangent of 0. With air as dielectric, the bandwidth is improved because the fields at the edges of the patch are less confined.

This thesis consists of analyzing a rectangular air-spaced patch antenna near 1800 MHz. The analysis consisted of designing two different patches using two different literatures; two patch antennas were simulated and built; the patch antennas parameters were measured and the results were compared with published literature. Patch antennas studies have not specifically investigated the air spaced case. Reported predictions indicate that for a microstrip patch antenna to deliver good results a dielectric of at least 2.2 should be used to build the antenna [2], [3].

## I.3 Summary of previous work

Literature found has studied a patch antenna with air gap in the dielectric or a patch antenna using foam. A patch antenna with an air layer in the dielectric is reported in [17]. The air layer is used to improve the performance of the antenna and the dielectric is important to reduce the antenna volume. This type of structure is used for GSM (Global System for Mobile communications) applications because they require the antenna to be very thin. The choice of foam as dielectric with lower permittivity ($\varepsilon_r$ = 1.03) is reported in [22]. It has been noted that foam is a porous material and the surface of the foam is not well defined. An air-spaced patch antenna case is described in [16]. However, in their approach, some design parameters are determined using simulation through commercial software. Without those parameters, computing the dimensions of the patch is not possible. Our approach is to use conventional equations as guidelines to

design the patch (to compute the dimensions of the patch). It will be shown here that a thorough study of the air-spaced patch antenna can result in the derivation of simple formulas for the patch design.

## I.4 Outline of the thesis

Chapter II of this work discusses the theory of microstrip antennas. The analysis, design and simulation tool for rectangular patches is also described in Chapter II. The simulation of air-spaced patch antennas is described in Chapter III. The simulation is used to analyze the air-spaced rectangular patch antenna and to provide guidelines about the experiment. Chapter IV discusses the experimental setup, various phases of the experiment, and the results obtained. A comparison between analytical, simulation and experimental results is discussed in Chapter V. A conclusion about the work done and future work are also described in Chapter V.

# Chapter II – Theory

## II.1 Patch Antenna Configurations

There are virtually an unlimited number of patch shapes for which radiation characteristics may be calculated. The basic configurations used in practice are:

- Square
- Rectangle
- Disk
- Ellipse
- Ring
- Pentagon
- Equilateral triangle

Their radiation characteristics are similar despite the difference in geometrical shape. Among the shapes listed, rectangular and circular patch antennas are widely used. Some particularities of other shapes compared to the rectangular shape are described below. [8]

- Square patches essentially provide only a circular polarization
- Circular disk microstrip elements may be easily modified to produce a range of impedances, radiation patterns and frequencies of operation
- Pentagon and elliptic structures provide circularly polarized radiation patterns using a single feed
- Triangular patches provide radiation characteristics similar to those of rectangular patches with a smaller size

## II.2 Rectangular Patch Antenna Theory

The rectangular shape of the microstrip patch antenna is the most used configuration and is the simplest patch structure. The substrate thickness is much less than a wavelength. A patch antenna can be analyzed using the transmission line model, the cavity model or the full-wave model. Patch antennas are typically used at frequencies ranging from 1 to 100 GHz. They are resonant antennas, which mean that they are usually operated near resonance in order to obtain real-valued input impedance.

The structure of a microstrip patch antenna is shown in Figure 1. A patch antenna consists of a single metal patch suspended over a ground plane. The two conductors are separated by a dielectric substrate. In Figure 1, $L$ is the length of the patch, $W$ is the width of the patch, and $h$ is the thickness of the dielectric substrate. Here the radiating patch is rectangular. A microstrip patch antenna near resonance has real input impedance, narrow bandwidth and a low to moderate gain.

Many substrate materials are used for microstrip antennas. The dielectric constant ranges from 1.17 to about 25 and the loss tangent ranges from 0.0001 to 0.004. Commercially available substrates include teflon/glass cloth ($\varepsilon_r = 2.5$), RT/duroid-5880 ($\varepsilon_r = 2.2$) and alumina ($\varepsilon_r = 9.8$). An air-spaced patch antenna can also be built and in this case the dielectric is air ($\varepsilon_r = 1$). Two approaches usually used for design of microstrip antennas with dielectric will be presented using the case $\varepsilon_r = 1$. These approaches are known to be inaccurate when the dielectric is air, so we will try to find a good correlation between the results and derive a conclusion from the analyzed problem.

## II.2.1 Design procedures for rectangular microstrip patch antenna

The goal of a design is to achieve specific performance characteristics at a specified operating frequency.

### II.2.1.1 Dimensions of the patch, effective length and effective width

Dimensions refer to the parameters for the design of the microstrip antenna structure. Let us define some terms which will be used in this section:

- c is the speed of the light in free-space
- $f_r$ is the resonant frequency
- $\varepsilon_r$ is the dielectric constant of the substrate
- $\lambda_0$ is the wavelength in free space
- $\lambda_d$ is the wavelength in the dielectric substrate

Energy is stored in the dielectric and the air. It is convenient to define an effective permittivity $\varepsilon_{eff}$ that accounts for both energies and allows for only one permittivity in the analysis. The effective permittivity also allows for an effective wavelength $\lambda_{eff}$.

The effective permittivity can be estimated using the formula: [2]

$$\varepsilon_{eff} = \frac{\varepsilon_r + 1}{2} + \frac{\varepsilon_r - 1}{2}\left[1 + \frac{h}{W}\right]^{-1/2} \quad (1)$$

where $W$ must be greater than $h$.

- Thickness of the substrate $h$

The choice of the dielectric substrate with an appropriate thickness is the first step in the design of the microstrip antenna. The thickness of the dielectric substrate is usually much smaller than one wavelength (on the order of 0.01), and it is usually chosen for the desired bandwidth.

- Patch element width $W$

The patch width has a minor effect on the resonant frequency and the radiation pattern of the antenna. It affects the input resistance and the bandwidth. The patch width also affects cross-polarization characteristics. The patch width is given by formula (2). [2]

$$W = \frac{c}{2f_r}\sqrt{\frac{2}{\varepsilon_r + 1}} \tag{2}$$

which is equal to $\lambda_0/2$ since $\varepsilon_r = 1$.

The patch width can also be selected to obtain good radiation efficiency.

- Patch element length $L$

The patch length determines the resonant frequency, and is a critical parameter in design because of the inherent narrow bandwidth of the patch.

The length can be found using two procedures:

- It can be chosen slightly less than a half-wavelength [3]. One choice is to express the length as:

$$L = 0.49\lambda_0 \tag{3}$$

- The length can also be found by calculating the extension length $\Delta L$ ([2], shown in Figure 2) of the patch and use it to determine $L$. The effective length of the patch is defined as:

$$L_e = L + 2\Delta L = \lambda_{eff}/2 \tag{4}$$

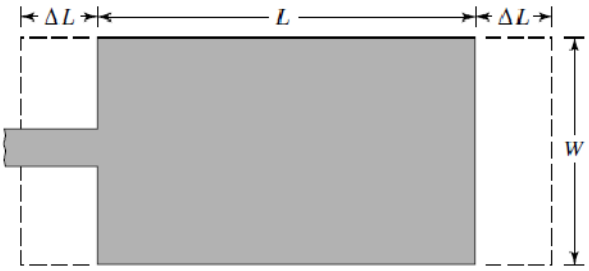


Figure 2: Top View of a microstrip patch element

In the air-spaced patch antenna case, $\lambda_{eff} = \lambda_d = \lambda_0$ .

$L$ can be derived as, $L = \lambda_0/2 - 2\Delta L$. The extension length is given by formula (5). [2]

$$\frac{\Delta L}{h} = 0.412\frac{\left(\varepsilon_{reff} + 0.3\right)\left(\frac{W}{h} + 0.264\right)}{\left(\varepsilon_{reff} - 0.258\right)\left(\frac{W}{h} + 0.8\right)} \tag{5}$$

- Recess feed distance $d$

Usually the input impedance at the edge of the patch is too large. The input impedance can be matched to 50 Ω by varying the feed location. As the feed point moves

from the edge of the patch toward the center, the impedance decreases till it reaches an impedance minimum. The impedance as a function of the feed location or the recess feed distance, for the rectangular microstrip element, is given by the formula (6) [3].

$$R_{in} = \frac{(120\lambda)^2 + \left(\frac{377h}{W\sqrt{\varepsilon_r}}\right)\left(\frac{tan^2(\beta d) + tan^4(\beta d)}{1 + tan^2(\beta d)}\right)}{240W\lambda\left(1 + tan^2(\beta d)\right)} \quad (6)$$

The 50-Ω-impedance point can be determined by solving for $d$, given $R_{in} = 50\Omega$. The corresponding distance is the recess distance, the distance from the edge of the patch toward the center. The feed element should be placed at this location.

### II.2.1.2 Common design procedures

Some parameters have to be specified in order to design the patch. Specified information includes the permittivity ($\varepsilon_{eff} = 1$), the resonant frequency ($f_r$), the height of the substrate ($h$), and the fact that $W$ has to be less than $L$ to avoid other resonances in the cavity model. Two common design procedures are established:

1) Procedure 1 [3]
    - Specify $f_r$ and $h$
    - Compute $L = 0.49\lambda$ using (3)
    - Choose $W$ less than $L$
    - Calculate the recess feed location by using (6)

2) Procedure 2 [2]

- Specify $f_r$ and $h$
- Determine $W$ by using (2)
- Determine $L$ by calculating $\Delta L$ and by using (5)
- Calculate the recess feed location by using (6)

### II.2.2 Transmission Line Model

The rectangular microstrip patch antenna can be modeled as a section of transmission line. The transmission line model represents the patch antenna as an array of two radiating slots separated by a low-impedance transmission line of a certain length. It is the easiest technique to analyze rectangular patch antennas but the least accurate.

#### II.2.2.1 Fringing effects

In practice, the fields are not confined to the patch. A fraction of the fields lie outside the physical dimensions $L \times W$ of the patch, because the dimensions are finite. This is called the fringing field. Since some of the waves travel in the substrate and some in the air (depicted in Figure 3), an effective permittivity is introduced to account for the fringing field along all the edges of the patch and the wave propagation in the patch.

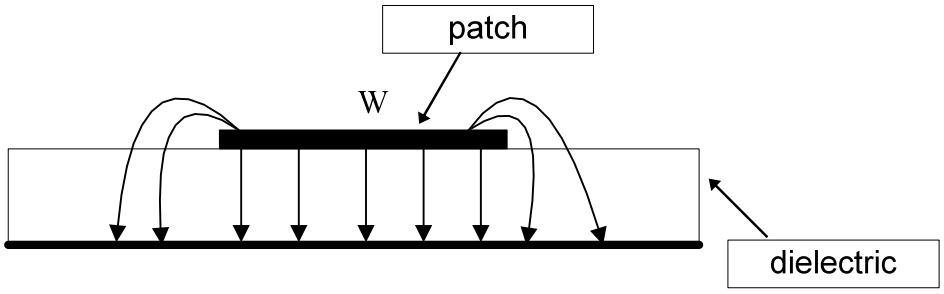


Figure 3: Electric field lines

The amount of fringing depends on the dimensions of the patch and the height of the dielectric substrate. Therefore the ground plane has to be big enough to support fringing fields in order to be acceptable. The effective permittivity $\varepsilon_{eff}$ is equal to the permittivity of the dielectric itself $\varepsilon_r$ , in the case of an air-spaced patch antenna, because the dielectric is air ($\varepsilon_r = 1$).

### II.2.2.2 Simple transmission line model

The simple transmission line model was the first technique used to analyze a rectangular microstrip antenna. It was developed by Munson in 1974 [13]. Here the dielectric is modeled as a section of transmission line (shown in Figure 5). The characteristic impedance $Z_0$ and the propagation constant β, for the line are determined by the patch size and the substrate parameters. A patch of dimensions $L \times W$ is shown in Figure 4. The periphery of the patch is described by four walls at $x = 0, L$ and $y = 0, W$. The four edges of the patch are classified as radiating slots or non radiating slots. The radiating slots (along $W$ or $x = 0, L$) are associated with slow field variation and the non radiating slots (along $L$ or $y = 0, W$) should have an integral multiple of half-wave variations along the edges ($L$ or $y = 0, W$), such that there is an almost complete

cancellation of the radiated power from the edge. In the far field, the electric field from the non radiating slots is very small and assumed negligible.

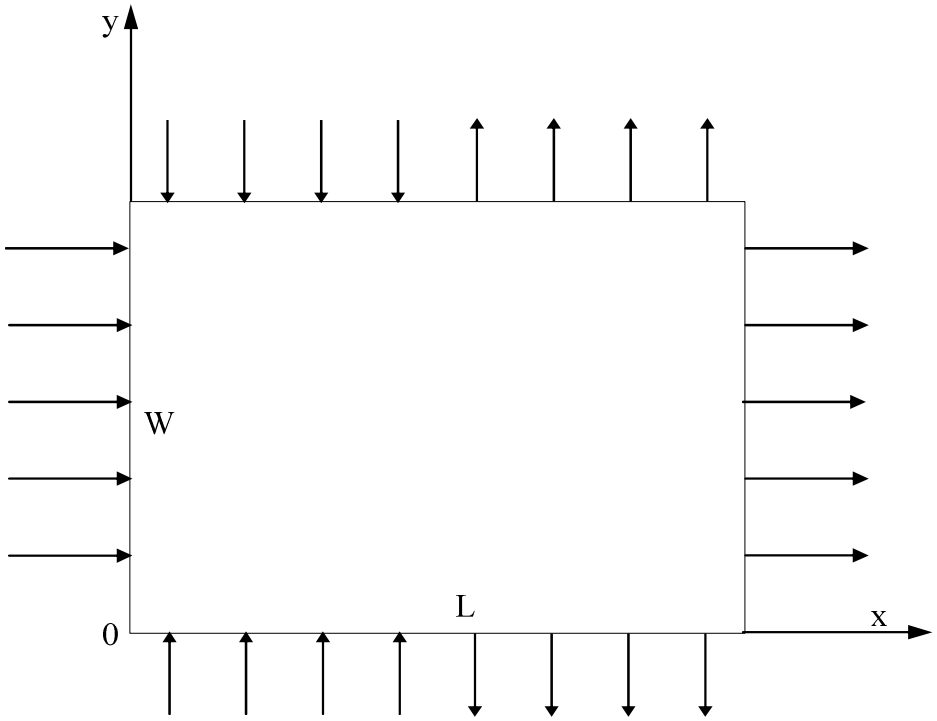


Figure 4: Fringing field along each slot of the patch antenna

The edges at $x = 0, L$ radiate most of the power and are characterized by admittances $Y_s = G_s + jB_s$ with s = 1, 2 (see Figure 5). $G_s$ is the conductance associated with the power radiated from the edge walls and $B_s$ is the susceptance due to the energy stored in the fringing field near the edge. $Y_c$ is the characteristic admittance of the patch fed (as a transmission line) at $x = L$. Since the edges in Figure 5 are identical, $Y_2 = Y_1$, $G_2 = G_1$ and $B_2 = B_1$.

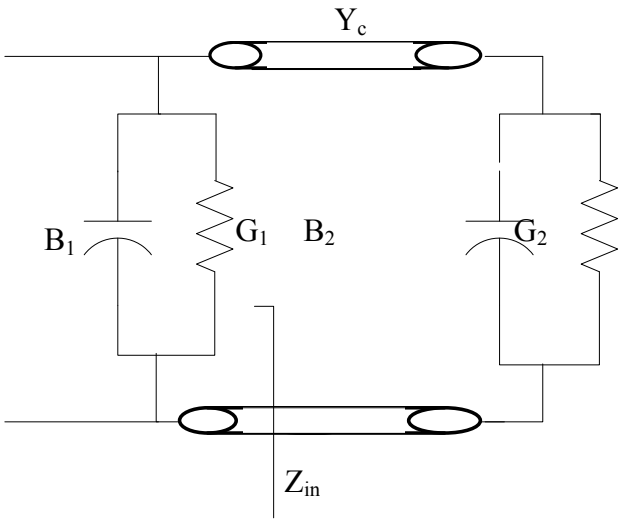


Figure 5: Transmission line model equivalent circuit

Using the model depicted in Figure 5, an expression for the resonant input impedance can also be found using (6). It is important to notice that this model is applicable for rectangular patch only and the effects of substrate and input reactance are not considered [2].

### II.2.3 Cavity Model

The cavity model is used to determine the normalized electric field within the dielectric substrate. The model considers the microstrip antenna as a cavity which means that the patch is over the ground plane and the two are separated by a dielectric substrate. The patch and the ground plane are considered as perfectly electric conductors and the edges of the dielectric substrate (walls of the cavity) as magnetic walls (perfectly magnetic conductors). These assumptions are based on the following observations for thin substrates ($h << \lambda$) (see Figure 6):

- The fields in the interior region do not vary along the x direction
- The electric field is x-directed only and the magnetic field has only the transverse components in the region bounded by the patch and the ground plane. This observation is used to assume that the top and the bottom of the cavity are electric walls.
- The electric current in the patch has no component normal to the edge of the patch, which implies that the tangential component of along the edge is negligible and a magnetic wall can be placed along the periphery.

When the microstrip patch is energized, a charge distribution is established on the upper and lower surfaces of the patch and on the surface of the ground plane. The charge distribution is controlled by an attractive and a repulsive mechanism. Most of the charge concentration and current flow remain underneath the patch because the attractive mechanism dominates. This dominance occurs because the height-to-width ratio is very small. The geometry of the microstrip patch for the cavity model is shown in Figure 6.

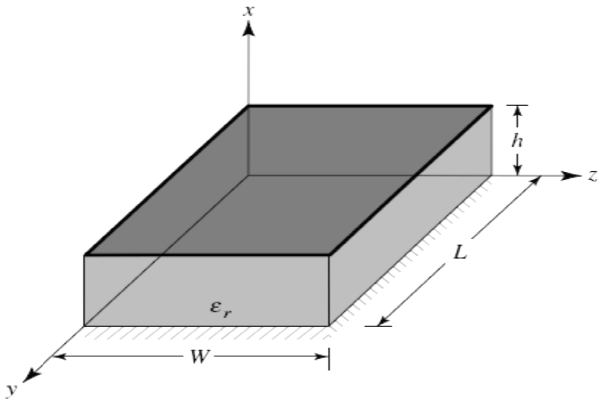


Figure 6: Rectangular microstrip geometry for the cavity model [2]

Since the height-to-width ratio ($h/W$) is small, the tangential magnetic fields at the edges would not be exactly zero but will be very small, and therefore an approximation made in the cavity model is to treat the side walls as perfectly magnetic conducting walls. The fields' configuration within the cavity can be found using the vector potential approach, equivalence principle and assuming that there is no fringing of the fields along the edges of the cavity. Considerations used to define the model are:

- Only field configurations will be considered within the cavity because fringing of the fields along the edges of the patch are very small ($h \ll \lambda$).
- Bottom and top of the cavity are considered perfectly electric conducting, and the four side walls are considered perfectly magnetic conducting.

Consider a $TM^x$ situation, then:

$$\vec{A} = A_x \hat{e_x} \tag{7}$$

The magnetic vector potential must satisfy the homogeneous wave equation:

$$\nabla^2 A_x + k^2 A_x = 0 \tag{8}$$

Using the separation of variables method, the analytic solution of the potential vector is found to be (9).

$$A_x = \left[A_1 \cos(k_x x) + B_1 \sin(k_x x)\right]\left[A_2 \cos(k_y y) + B_2 \sin(k_y y)\right]\left[A_3 \cos(k_z z) + B_3 \sin(k_z z)\right] \tag{9}$$

where $k_x$, $k_y$, $k_z$ are the wavenumbers along the x, y and z directions, respectively.

Using the boundary conditions:

$$E_y(0,y,z) = E_y(h,y,z) = 0$$
$$H_y(x,y,0) = H_y(x,y,W) = 0 \tag{10}$$
$$H_z(x,0,z) = H_z(x,L,z) = 0$$

The wave propagation numbers $k_x$, $k_y$, $k_z$ are derived.

$$B_1 = 0 \qquad k_x = \frac{m\pi}{h}, m = 0,1,2,...$$
$$B_2 = 0 \qquad k_y = \frac{n\pi}{L}, n = 0,1,2,... \tag{11}$$
$$B_3 = 0 \qquad k_z = \frac{p\pi}{W}, p = 0,1,2,...$$

This reduces the vector potential equation to:

$$A_x = \sum_{m=0}^{\infty}\sum_{n=0}^{\infty}\sum_{p=0}^{\infty} A_{mnp}\cos\left(\frac{m\pi}{h}x\right)\cos\left(\frac{n\pi}{L}y\right)\cos\left(\frac{p\pi}{W}z\right) \tag{12}$$

where m, n and p represent the number of half-cycle field variations along the x, y and z axis respectively. The electric field is related to the magnetic vector potential by the equation:

$$\nabla\times\nabla\times\vec{A} = j\omega\varepsilon\vec{E}$$
$$\nabla\times\vec{A} = \mu\vec{H} \tag{13}$$

An expression for electric field and magnetic field components using equation (9) is derived as follows:

$$E_x = -j\frac{1}{\omega\mu\varepsilon}\left(\frac{\partial^2}{\partial x^2}+k^2\right)A_x \qquad H_x = 0$$
$$E_y = -j\frac{1}{\omega\mu\varepsilon}\frac{\partial^2 A_x}{\partial x\partial y} \qquad H_y = \frac{1}{\mu}\frac{\partial A_x}{\partial z}$$
$$E_z = -j\frac{1}{\omega\mu\varepsilon}\frac{\partial^2 A_x}{\partial x\partial z} \qquad H_z = -\frac{1}{\mu}\frac{\partial A_x}{\partial y} \tag{14}$$

The electric and magnetic fields within the cavity are therefore:

$$E_x = -j\frac{\left(k^2-k_x^2\right)}{\omega\mu\varepsilon}A_{mnp}\cos\left(k_x x\right)\cos\left(k_y y\right)\cos\left(k_z z\right)$$
$$E_y = -j\frac{k_x k_y}{\omega\mu\varepsilon}A_{mnp}\sin\left(k_x x\right)\sin\left(k_y y\right)\cos\left(k_z z\right)$$
$$E_z = -j\frac{k_x k_z}{\omega\mu\varepsilon}A_{mnp}\sin\left(k_x x\right)\cos\left(k_y y\right)\sin\left(k_z z\right)$$

$$H_x = 0$$
$$H_y = -\frac{k_z}{\mu}A_{mnp}\cos\left(k_x x\right)\cos\left(k_y y\right)\sin\left(k_z z\right) \tag{15}$$
$$H_z = \frac{k_y}{\mu}A_{mnp}\cos\left(k_x x\right)\sin\left(k_y y\right)\cos\left(k_z z\right)$$

Amplitudes of the electric/magnetic field cannot be determined only with the cavity model. To account for radiation, a loss mechanism has to be introduced. The effective loss tangent parameter is one way of taking into account loss. The effective loss tangent is chosen appropriately to represent the loss mechanism of the cavity, and the cavity is therefore considered like an antenna.

Since the wavenumbers are subject to the constraint: $k_x^2 + k_y^2 + k_z^2 = \omega_r^2\mu\varepsilon$ (16)

The resonant frequencies for the cavity are given by the formula:

$$(f_r)_{mnp} = \frac{1}{2\pi\sqrt{\mu\varepsilon}}\sqrt{\left(\frac{m\pi}{h}\right)^2+\left(\frac{n\pi}{L}\right)^2+\left(\frac{p\pi}{W}\right)^2} \tag{17}$$

The dominant mode with the lowest resonant frequency is $TM^x_{010}$ mode because $h < W < L$. The electric field configuration for the $TM^x_{010}$ mode is shown in Figure 7.

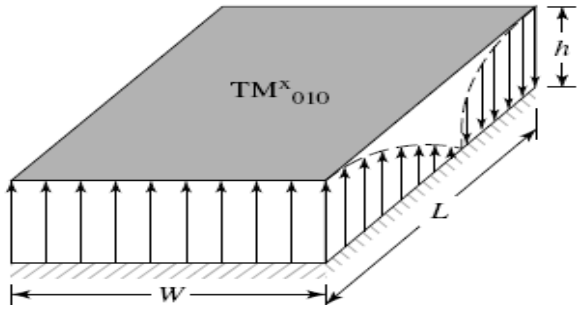


Figure 7: $TM^x_{010}$ mode for rectangular patch antenna [2]

We are using the $TM^x_{010}$ mode so field equations reduced to:

$$E_x = E_0\cos\left(\frac{\pi}{L}y\right), \qquad H_z = H_0\sin\left(\frac{\pi}{L}y\right)$$
$$E_y = E_z = H_x = H_y = 0$$
$$\text{where} \quad E_0 = -j\omega A_{010}, H_0 = (\pi/\mu L)A_{010}. \tag{18}$$

To determine the far field, the field equivalence principle is used. The microstrip is represented by an equivalent electric current density and the four side walls are represented by the equivalent electric current $J_s$ and equivalent magnetic current density $M_s$. Each slot is considered radiating the same fields as a magnetic dipole with current

density $M_s$. The far field produced by $\hat{n} \times \vec{E}_a$ over a closed surface, is the same as that produced by a surface magnetic current $\vec{M}_s$ over the same surface (see formula 19). Since the tangential electric field on the top and bottom faces, as well as the tangential magnetic field on the vertical surfaces, are zero, the only contribution to the equivalent sources are the tangential electric field $\vec{E}_a$, on the vertical surface of the cavity (see Figure 8). To account for the presence of the ground plane, image theory is used and it doubles the equivalent magnetic density current.

$$\vec{J}_S = 0, \qquad \vec{M}_S = -2\hat{n} \times \vec{E}_a \tag{19}$$

where $\hat{n}$ is the unit outward normal.

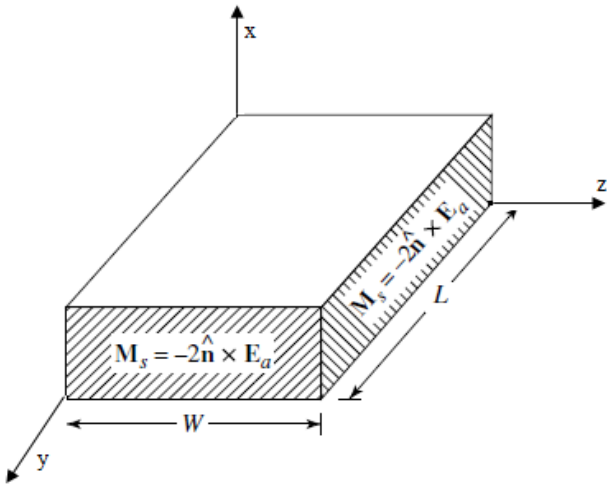


Figure 8: Equivalence principle equivalent [2]

The walls along the width (*W*) axis are called radiating slots because the equivalent magnetic current densities are both of same magnitude and of the same phase. Thus these sources add in a direction normal to the patch.

There are two orthogonal planes in the far field region. One is designated as E-plane and the other designated as H-plane. The far zone electric field lies in the E-plane and the far zone magnetic field lies in the H-plane. The E-plane is the x-y plane and the H-plane is the x-z plane (see Figure 8).

The two walls along the length ($L$) axis are called non-radiating slots because the equivalent magnetic current densities are of same magnitude but opposite phase. Thus the fields radiated by these two slots cancel each other in the H-plane. Because the corresponding slots on opposite walls are $180^o$ out of phase, the corresponding radiations cancel each other in the principal E-plane (see Figure 9).

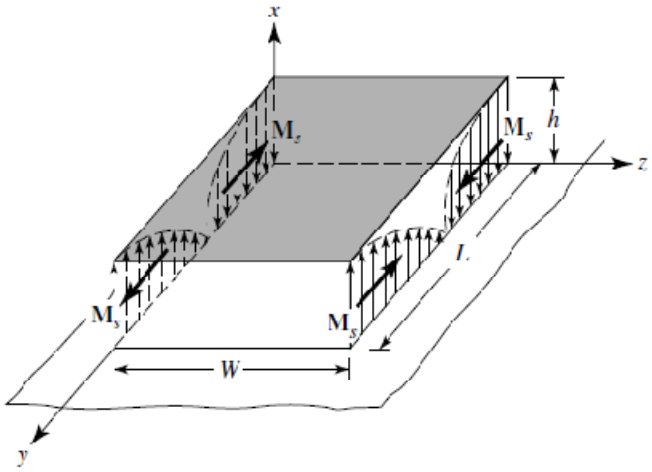


Figure 9: Current densities on non-radiating slots of rectangular patch antenna [2]

The far field is determined by considering only radiating slots. The antenna is therefore considered as two parallel radiating slots. The slots are identical, so the total electric field is the electric field of a two-element linear array. The electric field radiated by one slot is $E_1$ and the array factor is AF, so the product $E_1AF$ is the total electric field.

The method used to find the electric field $E_1$ on the radiating patch is similar to finding the electric field on a uniformly illuminated rectangular aperture.

### II.2.4 Feeding techniques

Matching between the feed line and the antenna can be achieved by properly selecting the location of the feed line, and this location also affects the radiation characteristics.

Many feed techniques can be used for microstrip antennas. The four most popular techniques are:

- Microstrip line feed: the microstrip line is a conducting strip, with width much smaller than the patch width (see Figure 10). The microstrip line feed is easy to fabricate, easy to match and simple to model.

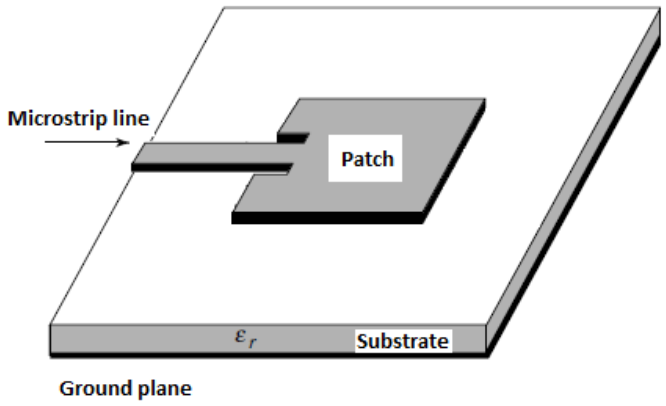


Figure 10: Microstrip antenna microstrip line feed

- Coaxial probe feed: it is a coaxial-line feed where the inner conductor of the coax is attached to the patch while the outer conductor is connected to the ground plane (see

Figure 11). The coaxial probe feed is easy to fabricate and to match but is difficult to model and requires soldering.

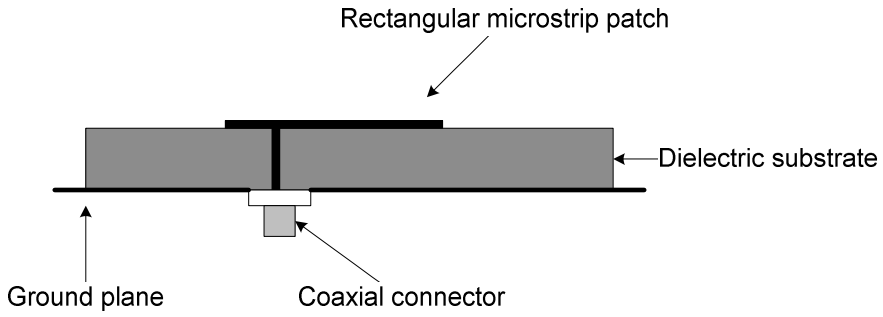


Figure 11: Microstrip antenna coaxial probe feed

- Aperture coupling: it consists of two substrates separated by a ground plane (see Figure 12). The microstrip feed line and the microstrip patch are located on different sides of the ground plane. The energy of the microstrip line is coupled to the patch through a slot on the ground plane. That is the reason why it is the most difficult to fabricate of all four techniques. Aperture coupling is easy to model and results in a narrow bandwidth. Matching is performed by controlling the width of the feed line and the length of the slot. [2]

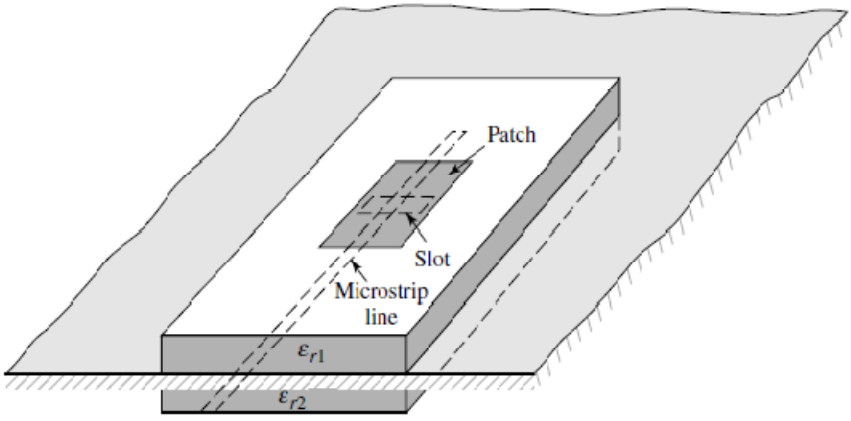


Figure 12: Microstrip antenna aperture-coupled feed

- Proximity coupling: the energy of the microstrip line is electromagnetically coupled to the patch through a second substrate (see Figure 13). Proximity coupling has the largest bandwidth of all four techniques, is easy to model and has low spurious radiation. The length of the feeding stub and the width-to-line ratio of the patch can be used to control the match. [2]

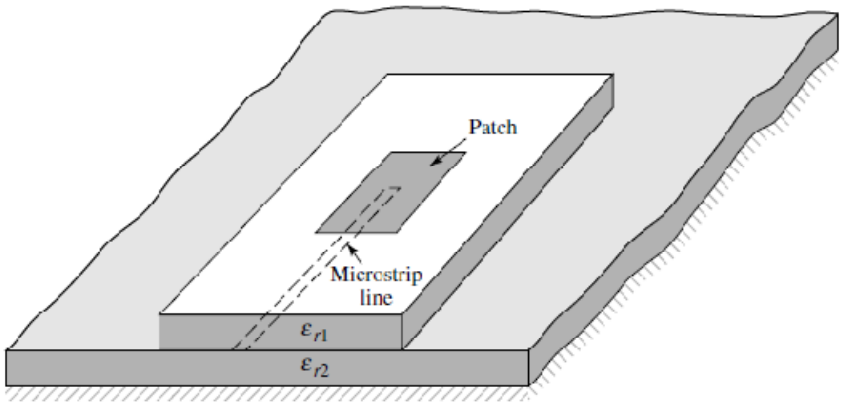


Figure 13: Microstrip antenna proximity-coupled feed

## II.3 Rectangular air-spaced patch antenna design

The goal is to have the antenna resonate at 1800 MHz, with a return loss of at least 10 dB and with air as the dielectric. From the common design procedures of section II.2.4, two different patch sizes have been computed. The center frequency is chosen to be 1800 MHz, which implies a wavelength $\lambda_0 = 16.66$ cm. The height should be between $0.003\lambda_0$ and $0.05\lambda_0$, it is chosen to be $0.03\lambda_0$ = 0.5 cm.

1) Procedure 1 [3]

- Length of the patch: $L = 0.49\lambda_0 = 8.17$ which is close to 8.2 cm

- Width of the patch: $W$ is chosen to be 7.6 cm
- Recess feed distance: using formula (6), $d = 2.5$ cm

2) Procedure 2 [2]

- Length of the patch: $\Delta L$ is computed from equation (5) and $\Delta L = 0.31$ cm then, $L = \lambda_0/2 - 2\Delta L = 7.6$ cm
- Width of the patch: $W$ is chosen to be 7 cm
- Recess feed distance: using formula (6), $d = 2.5$ cm

These two designs have been fabricated. Experimental results are discussed in chapter IV and chapter V.

## II.4 NEC Theory

The Numerical Electromagnetic Code (NEC) is the software used here to simulate the air-spaced patch antenna. The objectives of the simulation are:

- To obtain a better understanding of the design
- To provide a means of observing the results using various inputs

The simulation is expected to predict some characteristics of the experimental results. Accuracy is expected between the experimental results and the simulation results. Simulation results will be compared to experimental results.

### II.4.1 NEC Introduction

The Numerical Electromagnetic Code is an antenna modeling software package [12]. NEC was developed in 1970s at Lawrence Livermore laboratories. The code is based on the Method of Moments (MoM). The most recent version in public domain of NEC is NEC-2. While there are a number of excellent MoM codes available, NEC-2 is used in this work, because it is freely available and it is a powerful computational engine.

Structures are modeled in NEC through a grid of thin wires. Wires in NEC are modeled by short straight segments. The NEC solution is the current on the wire segments. From the currents, NEC can compute the far field radiation patterns, input impedances, and near fields.

In NEC, the current on each segment is represented by a constant, a sine and a cosine. The thin wire approximation considers that since the wire is very thin, the current density on each segment does not depend on the wire azimuthal angle □. The current density is only along the axis of the wire.

### II.4.2 Structure modeling guidelines

A wire segment in NEC is defined by the coordinates of its two end points and its radius. Simple ideas for modeling structures in NEC code use short and straight segments. Some guidelines are important to follow when modeling with NEC in order to obtain accurate simulation results: [13]

- The wire segment length $\Delta$ should be less than $0.1\lambda$ and greater than $0.001\lambda$ at the desired frequency

- The wire segment length $\Delta$ should be at least 4 times larger than the diameter *d* of the wire
- A wire should be at least nine segments per half-wavelength
- All segments length should be equal within a model as much as possible.
- Segments must not overlap
- Segments with small $2\Delta/d$ should be avoided at bends
- Segments that are electrically connected must have coincident end points. If the separation between the ends of two segments is less than 0.001 times the length of the shortest segment, the segments will be treated connected by the NEC code.
- The angle between two connected segments should not be extremely small to avoid overlaps
- Parallel wires should be several radii apart
- A segment is required at each point where a network connection or voltage source will be located

The guidelines given above are the most common sources of error in NEC, and it is important to test the accuracy of the results after simulation. It is also possible to generate inaccurate data due to other error sources.

Image theory is used in NEC to model an antenna over a ground plane. There are four types of ground plane in the NEC code:

- Perfectly conducting ground plane: here the code generates an image of the structure reflected on the ground plane. The image ground plane is infinite in this case. The image is exactly equivalent to a perfectly conducting ground plane.

The height in that case should be at least several times the radius for the thin-wire approximation to be valid.

- Finitely conducting ground plane: the image of the structure is generated and modified by the Fresnel plane-wave reflection coefficients. This method should not be used for structures close to the ground plane and is of limited accuracy.
- A wire ground screen may also be modeled using the Sommerfeld/Norton method when the structure is slightly raised above the ground plane.
- NEC also includes a radial-wire ground screen approximation and two-medium ground approximation based on modified reflections coefficient in the wire ground screen case.

# Chapter III – NEC Simulation

## III.1 Simulation setup

The rectangular patch antenna in NEC can be modeled as a rectangular mesh grid with precise number of segments. The ground plane is chosen to be perfectly conducting and infinite. The goal is the same as the one of section II.3: the antenna has to resonate at 1800 MHz, with a return loss of at least 10 dB and with air as dielectric.

An example of rectangular patch antenna modeled in NEC-2 is shown in Figure 14. The feed point is shown in red on Figure 14 and lies along the x-axis. The structure is at a height *h* from the ground plane (see Figure 15). The ground plane is the z = 0 plane (it is an infinite ground plane).

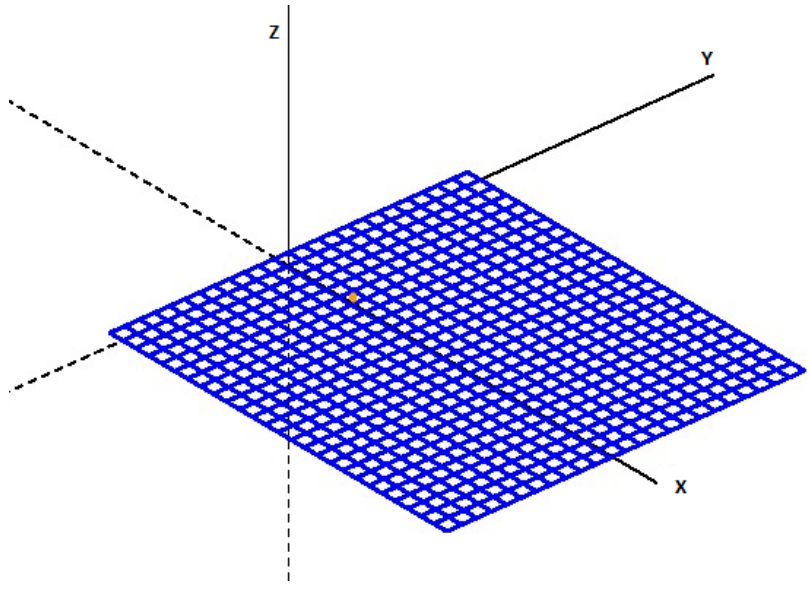


Figure 14: Geometry of microstrip patch antenna designed in NEC (3-D view)

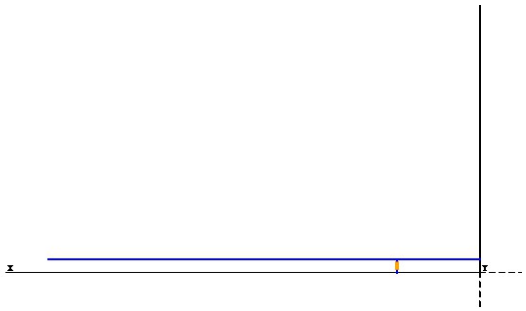

Figure 15: 2-D view (along the Y-axis) of the microstrip patch antenna in NEC

Two microstrip patch antennas were simulated in NEC at four different heights and at four different recess feed locations. The wire radius is set to 0.025cm. The dimensions of each square in the grid are a function of the patch size and the recess feed location. Table 1 is displayed below and shows an example of the dimensions of each square's grid versus recess feed location and the total number of segments for the two antennas at a height of 0.25 cm.

| Antenna | Recess feed location (cm) | $d_x$ (dimension along the x-axis) in cm | $d_y$ (dimension along the y-axis) in cm | Total number of segments |
|---|---|---|---|---|
| Antenna 1 L = 8.2 cm W = 7.6 cm | 1.5 | 0.3154 | 0.3166 | 1299 |
| | 2 | 0.3416 | 0.3455 | 1103 |
| | 2.5 | 0.3154 | 0.3166 | 1299 |
| Antenna 2 L = 7.6 cm W = 7 cm | 1.5 | 0.3166 | 0.3182 | 1103 |
| | 2 | 0.3454 | 0.3500 | 923 |
| | 2.5 | 0.3166 | 0.3182 | 1103 |

Table 1: Dimensions of the patch in the NEC simulation

It should be noted that all the guidelines listed in section II.3.2 are completely obeyed. The target frequency is 1800 MHz, which implies a wavelength of 16.66 cm. This means that the segment length should be chosen between 0.016 cm and 1.6 cm. The average length in this model is 0.3 cm. the radius of the wire is 0.025 cm which is much less than eight times the bigger segment length of 0.35 cm. all other conditions set for the guidelines are met.

In Table 1, $d_x$ represents the segment length along the patch width and $d_y$ represents the segment length along the patch length. A change in height (increase or decrease) will not affect the results of Table 1, it will just be a shift of the patch up or down, but will affect the results of the electric field or return loss. The dimensions of the grid do not depend on the patch size, but depend on the recess feed location distance. The simulation software tends to divide the wires in number of segments such that one will be crossing as close as possible to the feed segment.

## III.2 Simulation results

The experiment setup of the NEC simulation is presented in Table 2.

| Antenna | Recess feed distance (cm) | Height (cm) |
|---|---|---|
| Antenna 1<br>L = 8.2 cm<br>W = 7.6 cm | 1.5 | 0.25 |
| | | 0.5 |
| | 2 | 0.25 |
| | | 0.5 |
| Antenna 2<br>L = 7.6 cm<br>W = 7 cm | 2.5 | 0.25 |
| | | 0.5 |
| | 3 | 0.25 |
| | | 0.5 |

Table 2: Experiment setup of the NEC simulation

Table 2 shows the predefined parameters used in the simulation. For each patch of dimensions L × W, four recess feed distances (distance from the edge of the patch toward the center of the patch) are simulated: 1.5 cm, 2 cm, 2.5 cm and 3 cm. The recess feed distance of 3 cm is close to the zero impedance point; therefore it is not meaningful to go further than 3 cm. For each recess feed location, two heights (0.25 cm and 0.5 cm) are simulated. In total, each antenna has 8 simulation scenarios with an infinite ground plane. It has to be mentioned that the simulation is done using a step in frequency of 5 MHz. Measurements obtained for the NEC simulation are presented in Table 3.

| Antenna | Recess feed location (cm) | Height (cm) | Actual recess feed location (cm) | Center frequency (MHz) | $S_{11}$ (dB) |
|---|---|---|---|---|---|
| Antenna 1 L = 8.2 cm W = 7.6 cm | 1.5 | 0.25 | 1.5769 | 1700 | -3.631 |
| | | 0.5 | | 1685 | -8.477 |
| | 2 | 0.25 | 2.0500 | 1680 | -4.473 |
| | | 0.5 | | 1655 | -11.688 |
| | 2.5 | 0.25 | 2.5231 | 1675 | -8.123 |
| | | 0.5 | | 1635 | -30.854 |
| | 3 | 0.25 | 3.0750 | 1655 | -22.475 |
| | | 0.5 | | 1615 | -9.717 |
| Antenna 2 L = 7.6 cm W = 7 cm | 1.5 | 0.25 | 1.5833 | 1830 | -3.942 |
| | | 0.5 | | 1805 | -9.927 |
| | 2 | 0.25 | 2.0727 | 1805 | -5.348 |
| | | 0.375 | | 1760 | -9.858 |
| | | 0.5 | | 1770 | -15.828 |
| | | 0.6 | | 1750 | -29.858 |
| | 2.5 | 0.25 | 2.5333 | 1795 | -11.139 |
| | | 0.35 | | 1780 | -20.257 |
| | | 0.375 | | 1775 | -24.824 |
| | | 0.5 | | 1750 | -18.164 |
| | 3 | 0.25 | 3.1091 | 1770 | -12.271 |
| | | 0.5 | | 1725 | -4.772 |

Table 3: NEC simulation results

Table 3 indicates that antenna 1 in general, does not really lead to good results comparing all numbers. Some important conclusions that can be derived from Table 1 are:

- As the height increases, the resonant frequency decreases
- Results fail for d = 3 cm in most cases because it is very close to the zero impedance point (d = 3.5 cm)
- As the recess feed distance increases, the resonant frequency decreases
- A height of 0.25 cm is too short for the size of the patch antenna 1. It does not lead to the minimum return loss goal of 10 dB
- The smaller patch leads to better results compared to the larger patch

From Table 3, return loss values (- $S_{11}$(dB)) do not follow a particular trend as the height or the recess distance increases/decreases. For example for antenna 1, as the height increases, $S_{11}$(dB) decreases for d = 1.5, 2 and 3 but increases for d = 3 cm. In the simulation, return losses are not very accurate.

An example of NEC input and output files are presented in Appendix C. A plot example of the data for antenna 2, height = 0.25 cm and recess feed distance = 2.5 cm is shown in Figure 16. It shows the frequency along the horizontal axis and the return loss in dB along the vertical axis ($S_{11}$(dB) = 10 log($S_{11}$) and RL = - $S_{11}$(dB)). The graph shows the resonant frequency with the return loss maximum value at that peak frequency.

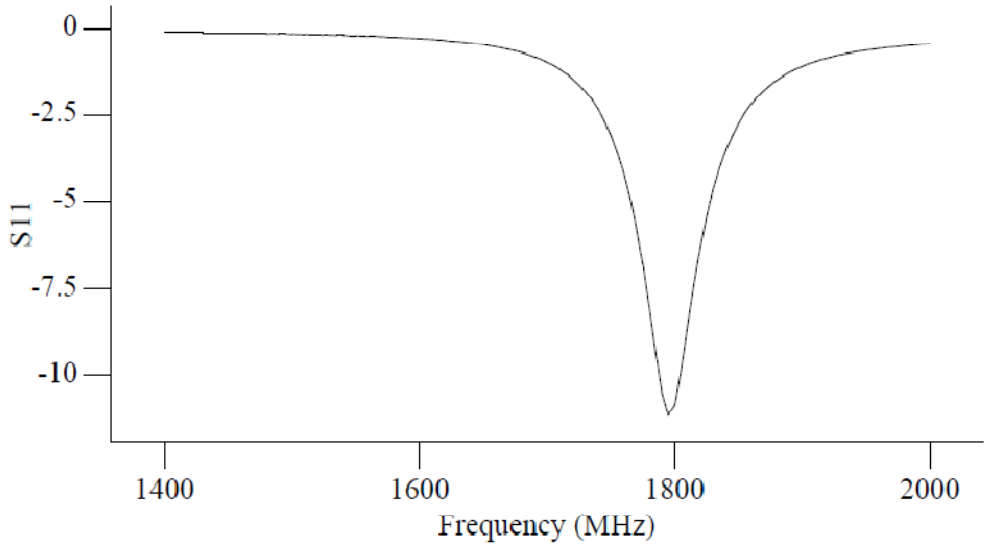


Figure 16: $S_{11}$ plot of antenna 2, patch size 7.6 cm × 7 cm, height 0.25 cm and recess feed distance 2.5 cm.

The antenna design predicts the best recess feed location at 2.5 cm. The couples (d = 2 cm, h = 0.5 cm) and (d = 2.5 cm, h = 0.25 cm), shown in Table 3 for antenna 2, depicts the best possible case scenarios. These two cases slightly modified are shown in Figure 17 and Figure 18. The idea is that the resonant frequency/maximum peak of the return loss should be as close as possible to the Smith chart origin for the antenna to be perfectly matched. If the minimum peak value of $S_{11}$(dB) is under the resistive line of the Smith chart, it means that the impedance is more capacitive. The height of the dielectric substrate in that case has to be increased to reduce the capacitance. Inversely, if the minimum peak value of $S_{11}$(dB) is above the resistive line of the Smith chart, it means that the impedance is more inductive. The height of the dielectric substrate in that case has to be decreased to reduce the inductance.

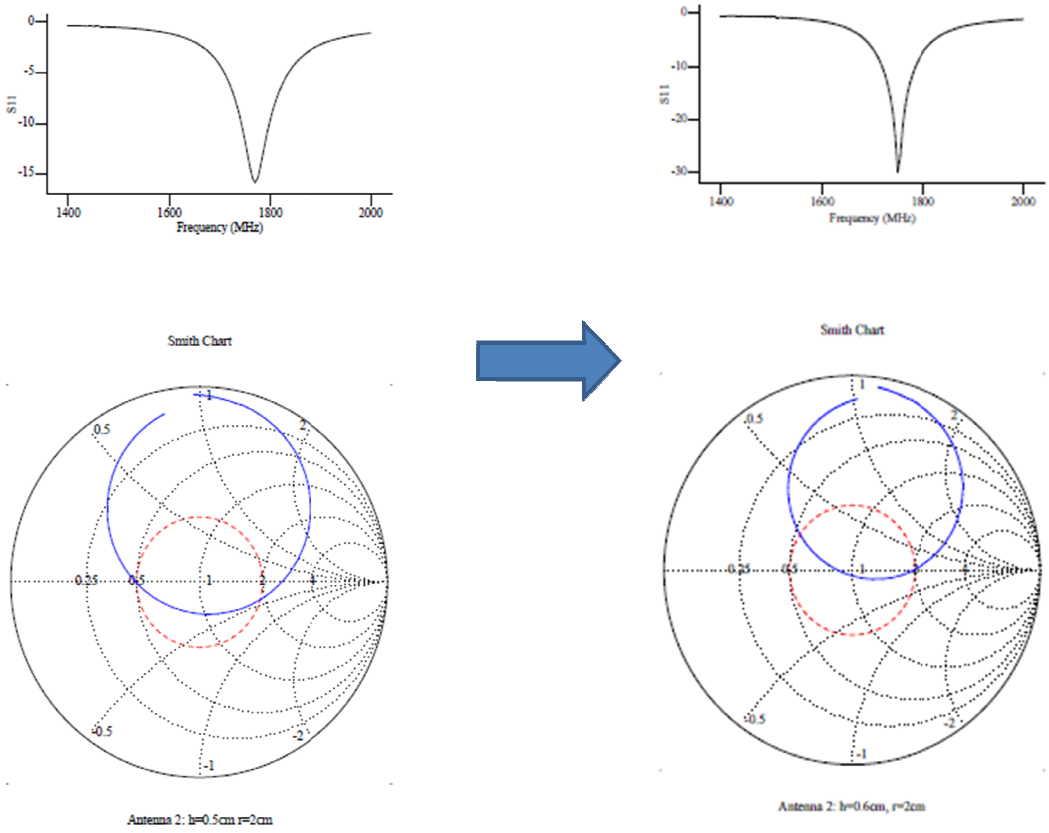


Figure 17: d = 2 cm, h = 0.5 cm case, modified in d = 2 cm, h = 0.6 cm

In Figure 17, above, the height is modified from 0.5 cm to 0.6 cm.

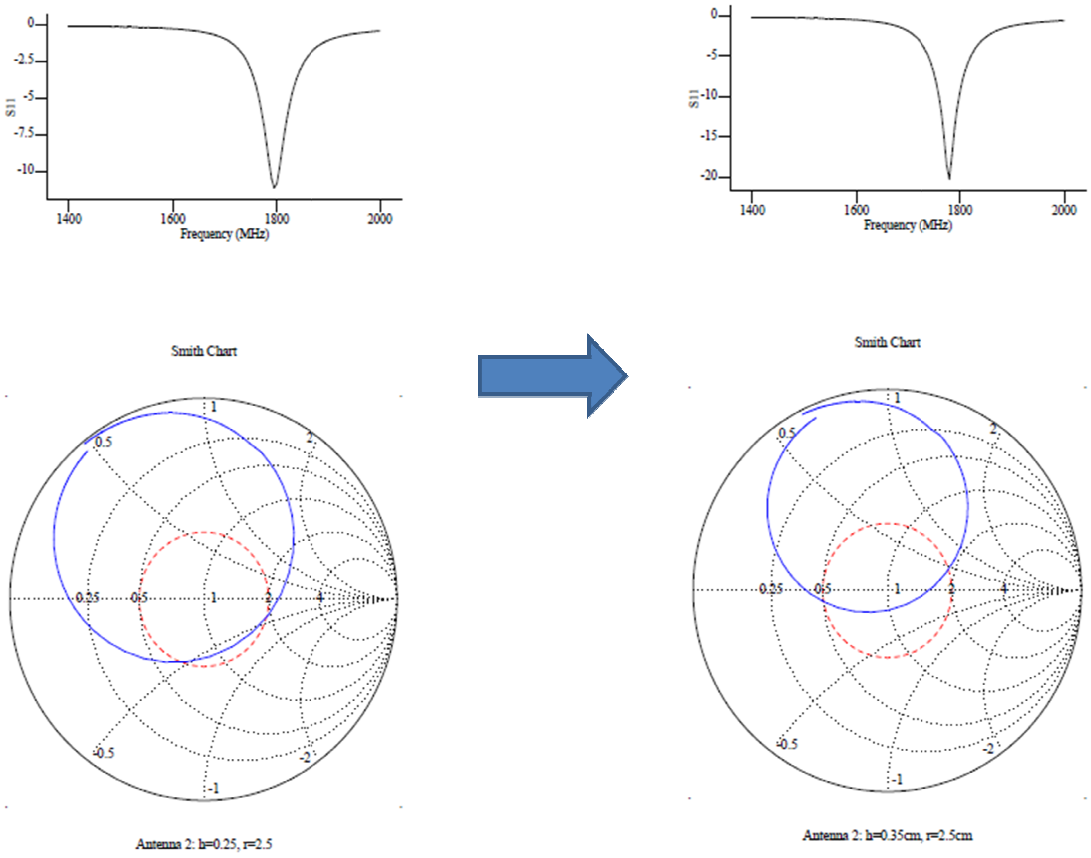


Figure 18: d = 2.5 cm, h = 0.25 cm case, modified in d = 2.5 cm, h = 0.35 cm

In Figure 17 and 18, the Smith charts of $S_{11}$(dB) are also shown. In Figure 17 and 18, it is seen on the left Smith charts that the $S_{11}$(dB) point corresponding to the resonant frequency is under the origin, which means that in order to improve the results; the height has to be increased in order to decrease the capacitance. The right pictures show the modification after an addition of 1 mm to the previous height and illustrate that the resonant frequencies are closer to the origin, which improves the return loss in that case but the resonant frequency value decreases by a small amount. In Figure 17, the height is modified from 0.25 cm to 0.35 cm.

# Chapter IV - Experimental results

## IV.1 Experiment setup

### IV.1.1 Material

Cost, power loss and performance were trade-off considerations in choosing the structure's material. After analysis of different metals, the formable brass (alloy 260) was chosen because it is easy to manipulate (cut and drill holes), affordable and performs well with many structures. The characteristics of the formable brass are:

- Hardness: Rockwell B60-B77, except 0.010" to 0.016" thicknesses are not rated
- Yield Strength: 52,000 psi
- Temper: 1/2 Hard (H02)

The brass sheet is 12mils thick which allows the thickness to be considered negligible. Other materials used to build the air-spaced patch antenna are:

- Nylon washers as spacers between the ground plane and the patch
- Household Glue used to hold the washers together in order to obtain a specific height and it is also used to attach the patch, the spacers and the ground plane together
- Solder iron and solder: they are used to attach the patch to the ground plane using the feed line
- Connectors: coaxial cable as feed line connector between the ground plane and the patch, male-female connector to be used to connect the antenna to the vector network analyzer

- Copper tape: it is used to tape the coaxial feed to the ground plane
- Vector Network Analyzer (VNA): To measure the $S_{11}$, the bandwidth and the Smith chart of the antenna. The one used is the Agilent 8714ES
- Discovery Learning Center (DLC): the DLC was used to cut the metal sheet into different pieces and to drill holes on the ground plane and the patch pieces

### IV.1.2 Methodology

The first step in the realization of the antenna is the design of the antenna using existing literature. After the antenna has been designed, materials were studied and/or chosen. Then the following steps were realized in order to build the antenna:

- ✓ Cut the patch antenna and the ground plane pieces at the Discovery Learning Center (DLC)
- ✓ Glue the washers together to obtain the desired height
- ✓ Mount the washers on the patch
- ✓ Mount the coaxial feed on the ground plane and make it stand vertically between the ground plane and the patch
- ✓ Use solder iron and solder to connect the coaxial feed and the patch
- ✓ Connect the patch to the Vector Network Analyzer and take measurements

### IV.1.3 Vector Network Analyzer

The Vector Network Analyzer (VNA) is a tool that measures the network parameters of a one port or two-port device/system. In order to be able to measure the

$S_{11}$, Smith chart and impedance of the antenna, the vector network analyzer has to be calibrated. A calibration kit should contain an ‘open’, a ‘short’ and a ‘load’. Because the only measurement taken is $S_{11}$, only one port is used. Steps for the calibration of the VNA are:

1) Set a frequency range: FREQ – START / STOP – number – MHZ
2) Calibrate the ports: CAL – Prior Menu – User 1-port – User 1-port

   Connect the Open to Port 1 and press Measure Standard

   Connect the Short to Port 1 and press Measure Standard

   Connect the Load to Port 1 and press Measure Standard

After those steps the VNA is calibrated for the frequency range defined in 1) and the VNA is ready to take measurements. Some other important functions of the VNA include:

- ✓ SCALE: to rescale the graph- Scale /Div or AUTOSCALE could be used
- ✓ FORMAT: Used to choose the display format Log Mag, Lin Mag, SWR, Delay, Phase, Smith chart, Polar, Real, Imaginary, and Impedance magnitude
- ✓ MARKER: To select either marker 1 or marker 2 as the active marker. You can also use the function ‘Marker Search’ to find the minimum or the maximum of a plot
- ✓ HARDCOPY: Press Start to be able to save pictures on a floppy disk

If the frequency range has to be changed a new calibration has to be performed. The calibration is not affected if the frequency range is modified and returned to the original range afterwards.

## IV.2 Experiment Results

The goal is still the same as in section II.3: the antenna has to resonate at 1800 MHz, with a return loss of at least 10 dB and with air as dielectric. The experiment setup in the laboratory is the same as the setup of Table 1. The ground plane is not an infinite ground plane and it is chosen to be $\lambda \times \lambda$ (16.66 cm × 16.66 cm) because it only has to be big enough to support fringing at the edge of the patch. Experiment was done in three phases.

The first phase consisted of testing both antenna 1 and antenna 2. In this experiment, the patch stands over the ground plane using nylon washers (as spacers) placed at the four corners of the patch. Results for phase 1 are presented in Table 4.

| Antenna | Recess feed location (cm) | Height (cm) | Center frequency (MHz) | SWR (dB) |
|---|---|---|---|---|
| Antenna 1 L = 8.2 cm W = 7.6 cm | 2 | 0.125 | 1600 | -16.3 |
| | | 0.25 | 1599 | -20.3 |
| | | 0.375 | 1562 | -26.6 |
| | | 0.5 | 1525 | -11.1 |
| | 2.5 | 0.125 | 1612 | -11.3 |
| | | 0.25 | 1600 | -17.1 |
| | | 0.375 | 1575 | -9.7 |
| | | 0.5 | 1525 | -8.2 |
| | 3 | 0.125 | 1575 | -11.6 |
| | | 0.25 | 1575 | -9.9 |
| | | 0.375 | 1525 | -6.3 |
| Antenna 2 L = 7.6 cm W = 7 cm | 2 | 0.25 | 1700 | -18.4 |
| | | 0.5 | 1637 | -8.8 |
| | 2.5 | 0.25 | 1687 | -10.7 |
| | | 0.5 | 1625 | -3.3 |
| | 3 | 0.25 | 1650 | -5.1 |
| | | 0.5 | 1712 | -8.0 |

Table 4: Experimental results of phase 1

Data from Table 4 shows that antenna 1, like in the simulation results, does not lead to good results. The highest resonant frequency for antenna 1 is 1612 MHz, which is 10.44% of error (relative error) compared to the goal frequency of 1800 MHz. Antenna 2 was therefore used for the rest of the experiments.

The second experiment consisted of re-testing antenna 2 for accuracy in the results with nylon washers still at the corners of the patch. Phase 2 results are presented in Table 5 and include measurements of the cases d = 2 cm, h = 0.6 cm and d = 2.5 cm, h = 0.35 cm.

| Antenna | Recess distance (cm) | Height (cm) | Center freq (MHz) | SWR (dB) |
|---|---|---|---|---|
| Antenna 2 L = 7.6 cm W = 7 cm | 2 | 0.25 | 1700 | -18.8 |
| | | 0.5 | 1637 | -9 |
| | | 0.6 | 1625 | -13 |
| | 2.5 | 0.25 | 1687 | -10.7 |
| | | 0.35 | 1650 | -8 |
| | | 0.5 | 1620 | -13.8 |

Table 5: Experimental results of phase 2

Here the calibration was also slightly modified to avoid having over 0 dB in some case shown in Figure 19. In phase 1, a male connector was included in the circuit after the calibration was completed to be able to connect the antenna to the Vector Network Analyzer (VNA). The calibration kit components (open, short, load) have male connectors at their ends, the VNA's cable connector is female and the antenna connector is female. So the calibration could not be done with the male connector because the calibration kit components also have male connectors. A load component of the calibration kit with female connector was found and the last step of the calibration was modified by including the male connector, connected to the VNA, at that step of the calibration. An example of measurement for the phase 2 is shown in Figure 20.

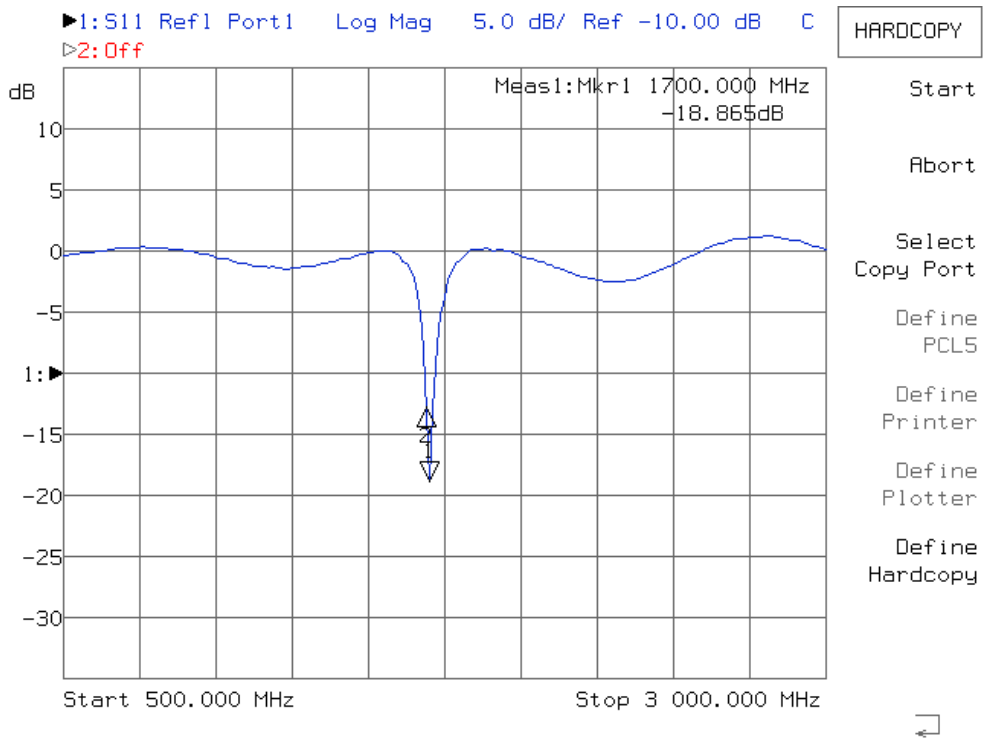


Figure 19: Example of measurement with incorrect calibration

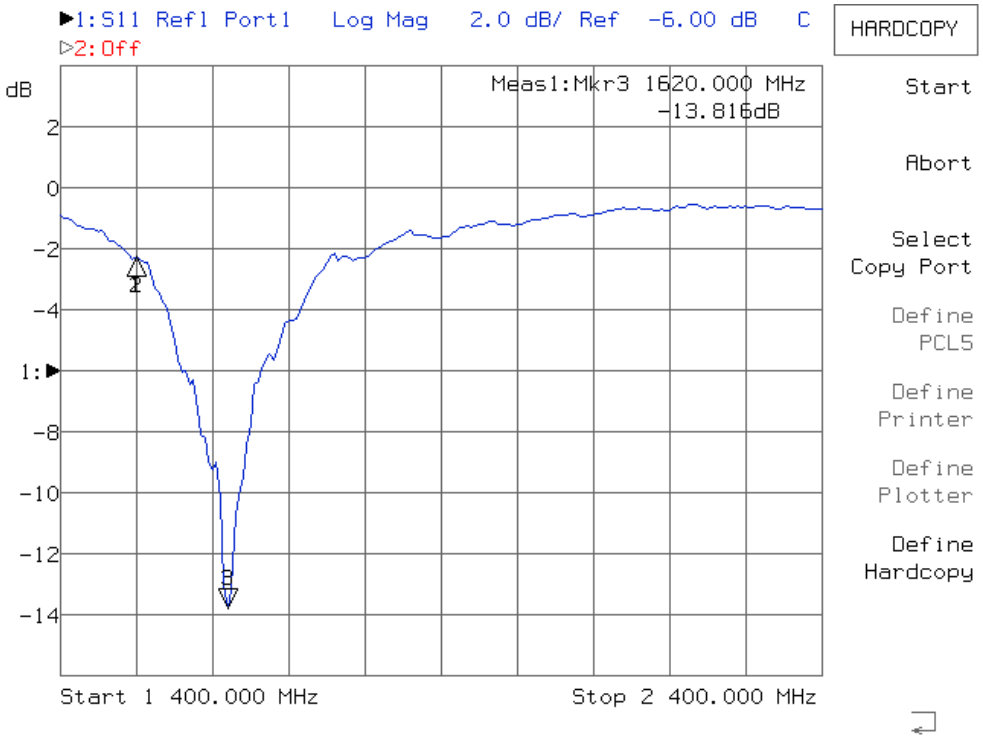


Figure 20: Example of measurement for phase 2 with improved calibration

Phase 2 experiments do not consider d = 3 cm. Table 4 indicates that the recess feed distance d = 3 cm does not lead to good results because the return loss goal of 10 dB is not reached in that case. It is probably due to the fact that it is close to the zero impedance point which is 3.5 cm.

A third experiment was conducted to find if the nylon washers placed at the corners of the patch have an influence on the fringing fields at the edges of the patch. For phase 3, the nylon washers were placed at the center of the patch where the impedance is null. The patch is fixed on the ground plane with the nylon washers. The phase 3 results are presented in Table 6.

| Antenna | Recess feed location (cm) | Height (cm) | Center frequency (MHz) | SWR (dB) |
|---|---|---|---|---|
| Antenna 2<br>L = 7.6 cm<br>W = 7 cm | 2 | 0.25 | 1800 | -21.5 |
| | | 0.375 | 1730 | -20.2 |
| | | 0.5 | 1680 | -17 |
| | 2.5 | 0.25 | 1760 | -13.5 |
| | | 0.375 | 1695 | -9.4 |
| | | 0.5 | 1645 | -7 |

Table 6: Experimental results of phase 3

An example of measurement for phase 3 is shown in Figure 21.

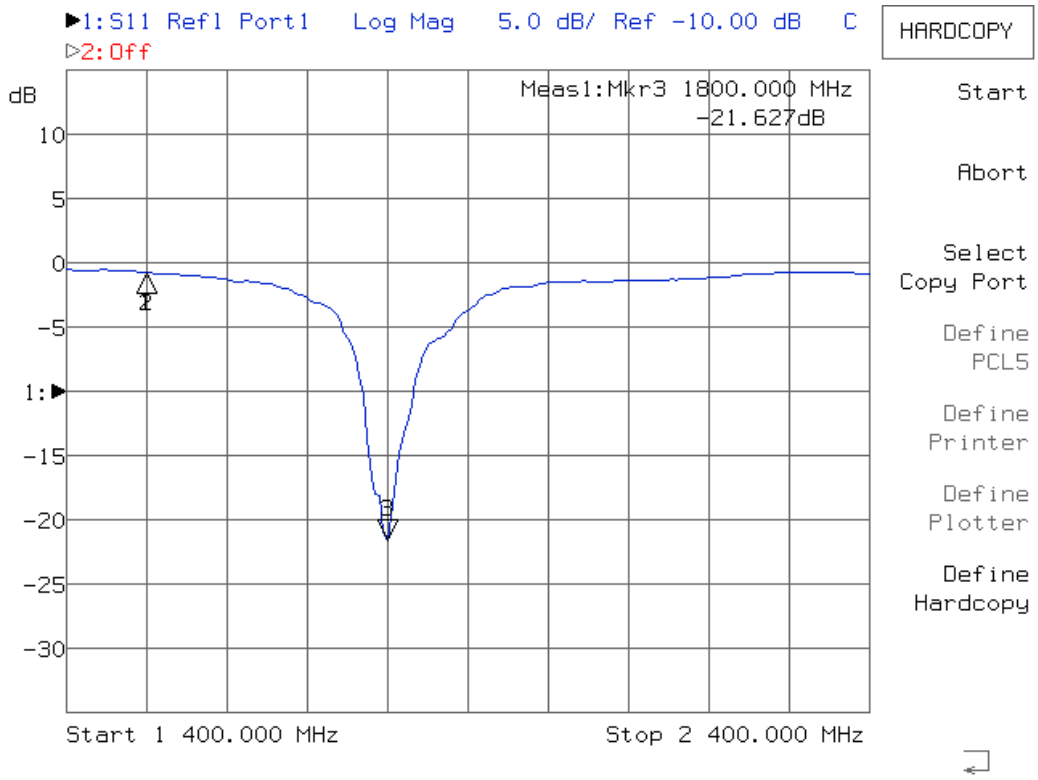


Figure 21: Example of measurement for phase 3

Phase 3 results were considered good enough to be the final results. They were considered final results because looking at Table 6, many results are pretty close to the goal. It is seen in Figure 21 that the maximum value of $S_{11}$ is under 0 dB. $S_{11}$ always under than 0 dB indicates an acceptable calibration. In Figure 19, 20 and 21, the peak indicates the resonance point. The corresponding frequency and return loss are the resonant frequency value and the maximum return loss value.

Table 6 illustrates that the case d = 2 cm, h = 0.25 cm has a resonant frequency of 1800 MHz and a return loss of 21.5 dB. d = 2 cm and h= 0.25 cm are not the values at which the antenna was designed (d = 2.5 cm and h = 0.5 cm) but lead to very good results. In the conclusion and discussion chapter, we will be comparing experimental and

simulation results, then we will try to explain the experimental results according to the initial designs and to the literature.

# Chapter V – Discussion, Conclusion and Future work

## V.1 Discussion

Analytic results are presented in Table 7. They are computed using procedure 2 from section II.3. A comparison between simulation and experiment results of antenna 2 are shown in Table 8 and Table 9. Simulation, experimental and analytic results are compared in Figure 22 and Figure 23.

| Height (cm) | Analytical results – Resonant frequency (MHz) |
|---|---|
| 0.25 | 1885 |
| 0.375 | 1845 |
| 0.5 | 1808 |

Table 7: Analytical results computed using procedure 2 from section II.3

| Height (cm) | Recess distance (cm) | Simulation results | | Experimental results | | Error (% to exp. freq) |
|---|---|---|---|---|---|---|
| | | Frequency (MHz) | $S_{11}$ (dB) | Frequency (MHz) | Return loss (dB) | |
| 0.25 | 2 | 1805 | -5.34 | 1800 | -21.5 | 0.27 |
| 0.375 | 2 | 1760 | -9.8 | 1730 | -20.2 | 1.67 |
| 0.5 | 2 | 1770 | -15.8 | 1680 | -17 | 5.35 |
| 0.25 | 2.5 | 1795 | -11.1 | 1760 | -13.5 | 1.98 |
| 0.375 | 2.5 | 1775 | -24.8 | 1695 | -9.4 | 4.72 |
| 0.5 | 2.5 | 1750 | -18.1 | 1645 | -7 | 6.38 |

Table 8: Comparison between simulation and experimental results

| Height (cm) | Recess distance (cm) | Simulation results | | Experimental results | | Difference of freq. (MHz) for a same height |
|---|---|---|---|---|---|---|
| | | Frequency (MHz) | $S_{11}$ (dB) | Frequency (MHz) | $S_{11}$ (dB) | |
| 0.25 | 2 | 1805 | -5.34 | 1800 | -21.5 | 10 \| 40 |
| 0.25 | 2.5 | 1795 | -11.1 | 1760 | -13.5 | |
| 0.375 | 2 | 1760 | -9.8 | 1730 | -20.2 | 15 \| 35 |
| 0.375 | 2.5 | 1775 | -24.8 | 1695 | -9.4 | |
| 0.5 | 2 | 1770 | -15.8 | 1680 | -17 | 20 \| 35 |
| 0.5 | 2.5 | 1750 | -18.1 | 1645 | -7 | |

Table 9: Table 8 re-ordered by heights

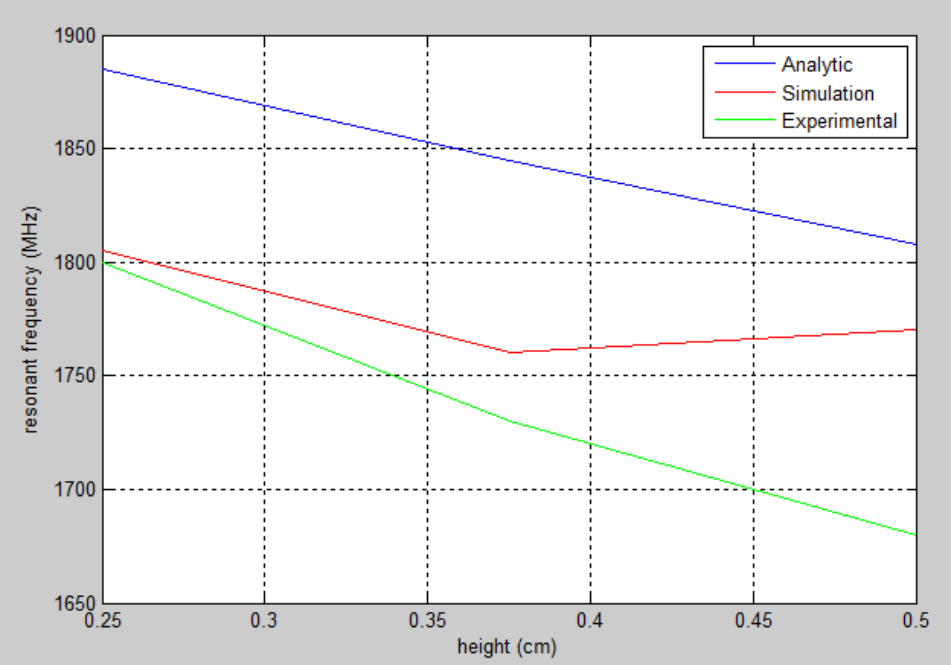


Figure 22: Picture of analytic, simulation and experimental results for d = 2 cm

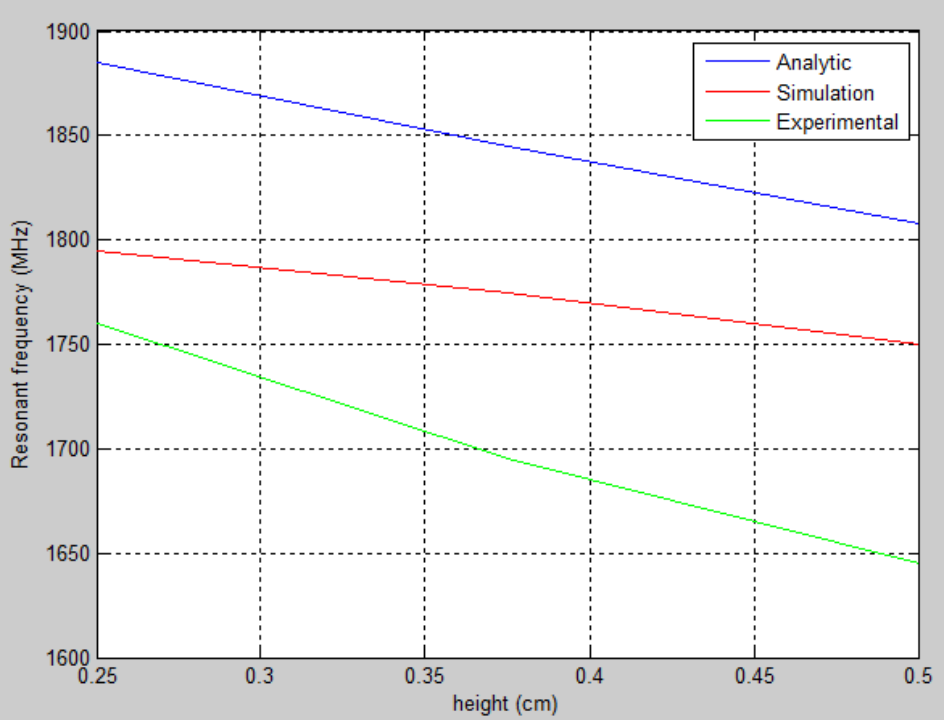


Figure 23: Picture of analytic, simulation and experimental results for d = 2.5 cm

Figure 22 and Figure 23 are the plots of analytic, simulation and experimental results for recess distances of 2 cm and 2.5 cm respectively. It is seen in those two pictures that the analytic results curve is very far off from the simulation and the experimental results curves. Another observation from the two figures is that the green curve (experimental results) and the blue curve (analytic results) are consistent. Analytical results are computed using procedure 2 (from section II.3) which is based on a literature [2] using experiments of microstrip patch antennas with dielectric to derive general equations and formulas. It is expected that in the case of air-spaced patch antennas, analytical results (due to experiments based equations) are not totally coherent with experiment results. It is seen in Figure 22 that the red curve (simulation results) does not perform well at h = 0.375 cm. One reason is the poor modeling of the case (d = 2 cm) which according to Table 1 has the lowest number of segments (923 segments). The patch is approximated with a mesh grid in the simulation and a finer grid will generally provide more accurate results.

It is seen in Table 7 that the resonant frequency in the analytic case does not depend on the recess distance. Table 9 indicates that there is a variation of the resonant frequency when the recess distance is changed. In the simulation results, the variation is approximately 15 MHz and in the experimental results, the variation is approximately 35 MHz. The return loss also decreases when the recess distance increases.

Table 8 indicates that the highest percentage of frequency error is 6.38%, and the error percentage increases with the height of the dielectric substrate for a specific recess distance. For a specific dielectric height, the error percentage also increases with the recess distance. Table 8 also illustrates that many error percentages are less than 5%

which are acceptable. The minimum error from Table 8 is 0.27% and it is obtained in the case d = 2 cm and h = 0.25 cm. It has to be remembered also that the calculation done using the literature predict the best case to be d = 2.5 cm and h = 0.5 cm. With more extensive research on the microstrip air-spaced patch antennas, equations and/or formulas can be derived from experiments to accurately predict the patch dimensions for a desired resonant frequency.

The differences between simulation results and experimental results (shown in Table 8) can be explained with different reasons:

- The ground plane is considered infinite in the simulation while it is of finite dimensions in the experiment
- The NEC model of the patch antenna is a grid mesh, while it is really a solid planar structure
- In the NEC model of the patch antenna, segments have a central unidirectional current; which means that current on top and at the bottom of each segment is the same. In the real patch antenna structure, the current and charge on top of the patch and the current and charge at the bottom of the patch are different (illustrated in Figure 24).

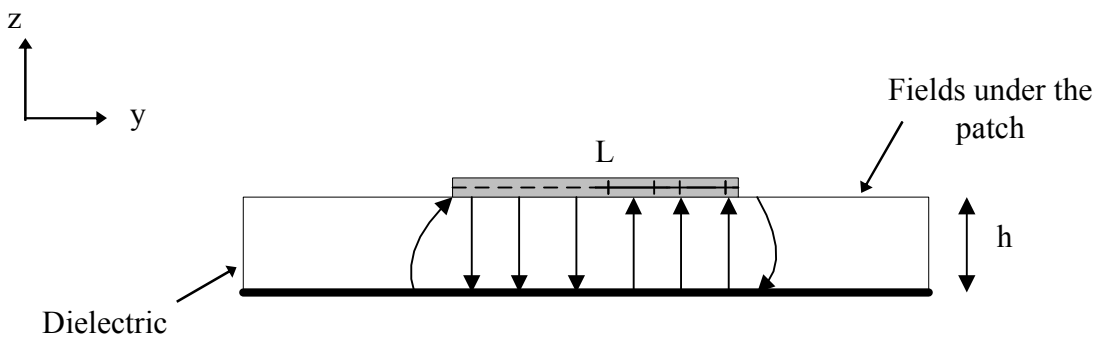


Figure 24: Side view of patch antenna with E-fields shown underneath

Many difficulties have been encountered during the practical realization of the antenna:

- Mechanical stabilization of the structure was very difficult to achieve, nylon washer are approximate but not quite accurate, and it is not proven that the glue permittivity and/or the nylon washer permittivity do not influence the effective dielectric constant
- The coaxial probe was soldered to the patch , and the soldering is not always reliable
- The Vector Network Analyzer (VNA) calibration was not precise. One reason is that the calibration kit has an ‘open circuit’ that is not very precise. Another reason is that calibration was done using two types of connectors for the same antenna (female (load); male (open and short)); the connector of the antenna is female and the VNA connector is female, so a male connector is included in the calibration but only at the load step because only a ‘load’ component with female connector was available.

It has to be mentioned that the brass conductivity was not included as a parameter of the simulation. A test was conducted to see the impact that the brass conductivity would have had on the simulation results. The comparison is recapitulated in Table 10.

| Antenna characteristics | | Resonant frequency | $S_{11}$(dB) |
|---|---|---|---|
| Antenna 2, h = 0.5 cm and d = 2 cm | Without brass | 1770 | -15.828 |
| | Brass included | 1770 | -16.203 |

Table 10: Comparison between two simulation results using the brass conductivity parameter or not.

Table 10 indicates that adding the brass conductivity as a simulation parameter would not have an impact on the resonant frequencies of Table 3. However, the bandwidths and the return losses of Table 3 will all change if the brass conductivity is taken into account.

Table 8 and Table 9 illustrate that experimental results were pretty satisfying and simulation results do not completely follow the experimental results trend for the resonant frequency case. Return loss values for simulation and experimental results were not compared due to the fact that parameters such as brass conductivity were not taken into account during the simulation.

## V.2 Conclusion

The goal was to analyze (design, simulate, build and measure the parameters of the antenna) an air-spaced patch antenna near 1800 MHz with a return loss of at least 10dB and matched at 50 Ω. Goal was set to be able to put a tradeoff limit on acceptable results. The predicted values, from the calculation using the literature, are d = 2.5 cm and h = 0.5 cm. The best values found using simulation and experimental results are d = 2 cm and h = 0.25 cm.

In the experimental results, as the height increases, the return loss and the resonant frequency decrease. Simulation results mostly follow that trend. The bandwidth and the return loss have the same trend. As the return loss increases, the bandwidth increases and vice versa.

Experiment lead to good results as shown in Table 8. Figure 22 and Figure 23 show that the analytical results and the experimental results are not close. It is normal because procedure 1 and procedure 2 (from section II.3) are based on the literature which used experiment of microstrip patch antennas with dielectric to derive general equation and formulas. Extensive experiments on the air-spaced patch antenna case can also lead to general equations and formulas.

## V.3 Future work

The focus of this thesis was to analyze an air-spaced patch antenna. Throughout the course of the analysis, simulation and experimentation were helpful to eliminate some cases and focus the analysis on specific cases to study. The present literature discusses

with microstrip patch antennas using a dielectric substrate. This thesis has analyzed an air dielectric case. However, a more precise fabrication of the antenna would result in a more mechanically stable structure than the one done by hand in the laboratory. Appendix D shows photographs of the air-spaced patch antenna constructed in this work.

Additionally, parameters of the antennas such as gain, radiation efficiency and radiation patterns have not been measured due to a lack of adequate equipment. An in-depth analysis of those parameters will provide a better characterization of the antenna. Also, more simulations of the air space patch antennas might provide derivation of equations or formulas for microstrip patch antennas with air dielectric. Most of the literature states that a dielectric permittivity less than 2.2 is not recommended for the antenna to be well designed [3], [2]. A better simulation will also improve the quality of the results by having results that can accurately compare to experimental results. Simulation can be improved by using commercial softwares, which are more precise than NEC and are able to simulate many other parameters of the antenna such as near fields, far fields and radiation pattern.

Lastly, the microstrip air-spaced patch antenna could be tested in one of the multiple applications mentioned in the thesis, to provide some detailed notes and guidelines about the practical use of the antenna. Theoretically, it is suggested that the air-spaced patch antenna might provide better results than microstrip patch antennas with dielectric.

## Bibliography

[1] W. L. Stutzman and G. A. Thiele, *Antenna Theory and Design*, John Wiley & Sons, Second Edition, New York, 1998.

[2] C. A. Balanis, *Antenna Theory – Analysis and Design*, John Wiley & Sons. Third Edition, New York, 2005.

[3] R. C. Johnson, *Antenna Engineering Handbook*, Third Edition, McGraw-Hill Book Company, New York, 1993.

[4] K. C. Gupta and Abdelaziz Benalla, *Microstrip Antenna Design*, Artech House, Norwood, 1988.

[5] I. J. Bahl and P. Bhartia, *Microstrip Antennas*, Artech House, Dedham, 1980.

[6] D. M. Pozar, *Microwave Engineering*, Addison-Wesley, Reading, 1990.

[7] K. F. Lee and W. Chen, *Advances in Microstrip and Printed Antennas*, John Wiley & Sons, New York, 1997.

[8] R. Garg, P. Bhartia, I. Bahl and A. Ittipiboon, *Microstrip Antenna Design Handbook*, Artech House, Boston, 2001.

[9] D. G. Fang, *Antenna Theory and Microstrip Antennas*, CRC Press Taylor & Francis Group, Boca Raton, 2010.

[10] K. F. Lee and K. M. Luk, *Microstrip Patch Antennas*, Imperial College Press, London, 2011.

[11] J. R. James, P. S. Hall and C. Wood, *Microstrip Antenna: Theory and Design*, Peter Peregrinus Ltd., London, 1981.

[12] J. Burke, and A. J. Poggio, *Numerical Electromagentics Code (NEC) - Method of Moments Part 1, 2, and 3*, Naval Ocean Systems Center, San Diego, CA, in Report NOSC TD 116, Jan. 1980.

[13] J. Richie, "The Numerical Electromagnetics Code, NEC", Marquette University Electromagnetic Simulation Laboratory, Report 23, Milwaukee WI, June 1999.

[14] R. E. Munson, "Conformal Microstrip Antennas and Microstrip Phased Arrays" *IEEE transactions on Antennas and Propagation*, Vol. AP-22, pp. 74-78, 1974.

[15] Dr A. Kumar, "Microstrip Antennas Guide Satellite Data Transmission", ED Online ID #10756, July 2005.

[16] D. Guta, S. Chattopadhyay and J. Y. Siddiqui, "Estimation of Gain Enhancement Replacing PTFE by Air Substrate in a Microstrip Patch Antenna", *IEEE Antennas and Propagation Magazine*, Vol. 52, pp. 92-95, June 2010.

[17] K. Wong, Y. Lin and B. Chen, "Internal Patch Antenna with a Thin Air-Layer Substrate for GSM/DCS Operation in a PDA Phone", *IEEE Transactions on Antennas and Propagation*, Vol. 55, pp. 1165-1172, April 2007.

[18] D. H. Schaubert, D. Pozar and A. Adrian, "Effect of Microstrip Antenna Substrate Thickness and Permittivity: Comparison of Theories with Experiment", *IEEE Transactions on Antennas and Propagation*, Vol. 37, pp. 677-682, June 1989.

[19] E. Elvine, G. Malamud, S. Shtrikman and D. Treves, "A Study of Microstrip Array Antennas with the Feed Network", *IEEE Transactions on Antennas and Propagation*, Vol. 37, pp. 426-434, April 1989.

[20] M. T. Islam, M. N. Shakib, N. Misran and T. S. Sun, "Broadband Microstrip Patch Antenna", *European Journal of Scientist Reasearch*, Vol. 27, pp. 174-180, 2009.

[21] R. A. Abd-Alhameed, D. Zhou, C. H. See and P. S. Excell, "A Wire-Grid Adaptive-Meshing Program for Microstrip-Patch Antenna Designs Using a Genetic Algorithm", *IEEE Antennas and Propagation Magazine*, Vol. 51, N$^{o}$ 1, pp. 147-151, February 2009.

[22] S. D. Targonski, R. B. Waterhouse and D. M. Pozar, "Design of Wide-Band Aperture-Stacked Patch Microstrip Antennas", *IEEE Transactions on Antennas and Propagation*, Vol. 46, N$^{o}$ 9, pp. 1245-1251, September 1998.

# APPENDIX A: Symbols and Notations

$\varepsilon_o$ = permittivity of free space and $\varepsilon_r$ is the permittivity in the medium

$\lambda$ = wavelength and is equal to phase velocity of the wave divided by the frequency in the medium

$S_{11}$ = reflection coefficient

$\beta = 2\pi/\lambda$, wave number

$\vec{A}$ = magnetic vector potential

$\vec{E}$ = electric field vector

$\vec{H}$ = magnetic field vector

$\omega$ = the angular velocity

# APPENDIX B: Parameters of the microstrip patch antenna

| Parameter | Formula |
|---|---|
| Effective dielectric constant, $\varepsilon_{reff}$ (1) | $\varepsilon_{reff} = \frac{\varepsilon_r + 1}{2} + \frac{\varepsilon_r - 1}{2}\left[1 + 12\frac{t}{W}\right]^{-1/2}$ |
| Width, W (2) | $W = \frac{c}{2f_r}\sqrt{\frac{2}{\varepsilon_r + 1}}$ |
| Normalized extension length, $\frac{\Delta L}{\mathrm{h}}$ (5) | $\frac{\Delta L}{h} = 0.412\frac{(\varepsilon_{reff} + 0.3)\left(\frac{W}{t} + 0.264\right)}{(\varepsilon_{reff} - 0.258)\left(\frac{W}{t} + 0.8\right)}$ |
| Length, L (3), (4) | $\lambda_d/2 - 2\Delta L$<br>$0.49\lambda_d$ |
| Effective length, Le (4) | $\frac{\lambda_d}{2} = \frac{\lambda_0}{2\sqrt{\varepsilon_r}}$ |

# APPENDIX C: Example of NEC input and output files (partial listing)

## Input file

Antenna 2: Patch dimensions L = 7.6 cm, W = 7 cm, h = 0.25 cm and d = 2.5 cm

```
CM Nw=22, L=7.600000, W=7.000000, h=0.250000, radius=0.025000
CM NL=24, dx=0.316667, dy=0.318182, shiftY=-3.500000
CE all dimensions are centimeters
GW 1 1 0.000000 -3.500000 0.250000  0.000000 -3.181818 0.250000  0.025000
GW 2 1 0.000000 -3.181818 0.250000  0.000000 -2.863636 0.250000  0.025000
GW 3 1 0.000000 -2.863636 0.250000  0.000000 -2.545455 0.250000  0.025000
GW 4 1 0.000000 -2.545455 0.250000  0.000000 -2.227273 0.250000  0.025000
.
.
.
GW 1102 1 7.283333 3.500000 0.250000  7.600000 3.500000 0.250000  0.025000
GW 1103 3 2.533333 0  0  2.533333  0 0.250000  0.025000
GS 0 0 0.01
GE 1 0
GN 1
FR 0 121 0 0 1400.000000 5.000000
EX 0 1103 2 1 1.0 0.0
XQ
EN
```

## Output file

Antenna 2: Patch dimensions L = 7.6 cm, W = 7 cm, h = 0.25 cm and d = 2.5 cm

| Frequency | Real imp | Img imp | SWR (dB) |
|---|---|---|---|
| 1400.000000 | 0.373974 | 24.068700 | -0.105488 |
| 1405.000000 | 0.381483 | 24.277900 | -0.107254 |
| 1410.000000 | 0.389298 | 24.481400 | -0.109101 |
| 1415.000000 | 0.397578 | 24.681900 | -0.111068 |
| 1420.000000 | 0.406151 | 24.892500 | -0.113084 |
| 1425.000000 | 0.414854 | 25.102500 | -0.115119 |
| . | | | |
| . | | | |
| . | | | |
| 1995.000000 | 1.589620 | 23.417700 | -0.452972 |
| 2000.000000 | 1.551800 | 23.770000 | -0.43979 |

## APPENDIX D: Air-spaced patch antenna pictures

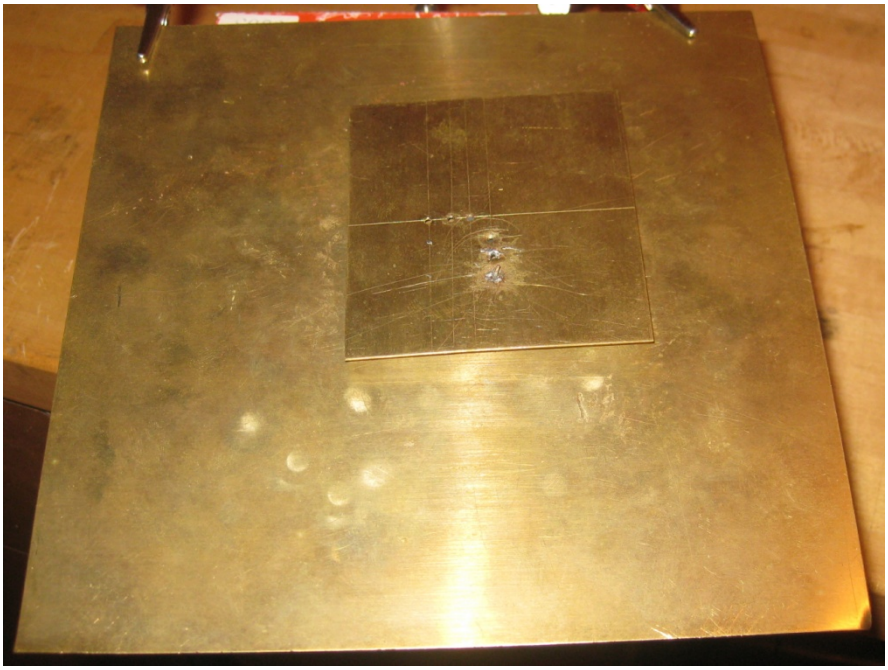

Air-spaced patch antenna built in the RF laboratory of Marquette University - Top view

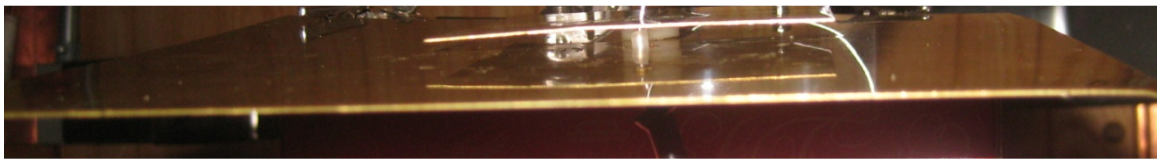

Air-spaced patch antenna built in the RF laboratory of Marquette University – Side view